Chapter 3

Instrumentation

3.1 SPHERE

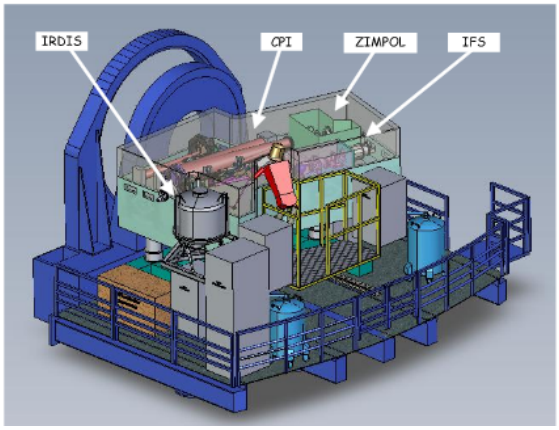

(a) Figure adapted from [17]

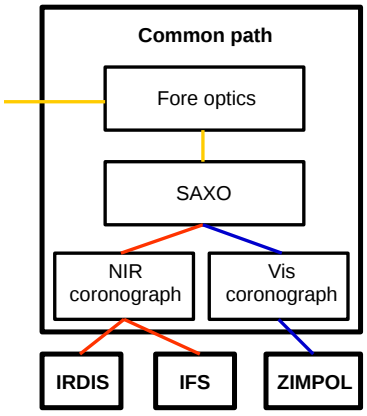

(b)

Figure 3.1: *overview of SPHERE*

SPHERE is an instrument for the VLT which is optimized for high contrast imaging. The instrument is placed in the Nasmyth of Unit Telescope 3 (UT3), one of the main VLT units, as illustrated in Figure 3.1. The instrument can be split up into four systems, the common path optics and three subsystems, IRDIS, IFS and ZIMPOL. ZIMPOL (Zurich Imaging POL arimeter [18]) uses visible light and IRDIS and IFS both near infrared light (NIR). Since IRDIS and IFS can work in parallel by use of a dichroic beamsplitter, we will discuss IRDIS briefly and take some time to look at the IFS

in detail.

3.1.1 Common path

The common path (CPI) is the main system of SPHERE that powers all the cryostats and motors, corrects the light for many distorsions and connects all the sub-systems to the light path. SAXO (Sphere Adaptive optics for eXoplanet Observation [19]) plays an important role in the correction of the incomming light in CPI. Part of CPI are the coronagraphs that can be included in the light path for further improvement of the final result.

pupil stabilizing fore optics

SPHERE has a derotater that is able to stabilize the field and the pupil on the detector. This stabilization is needed because of the rotation of the earth around its axis. The rotation of the earth causes a rotation of the field due to a change in parallactic angle and altitude of the object and a rotation of the telescope pupil with respect to the instrument due to the change in altitude of the object that is observed. The pupil has an offset with respect to the true north of -135.99^o, which means that all the data taken with SPHERE has to be rotated with that angle in order to make sure that north is pointing up. The field of view of the IFS is for technical reasons rotated with respect to the IRDIS field of view by 100.48$\pm$0.10^o. The data in our dataset has hence to be rotated with a total offset of -35.51^o in order to make sure that the north is pointing up[20].

After entering the instrument, the light path is protected against many possible noise sources. The vibrations in the Nasmyth platform that are caused by seismic activity or other reasons are damped by use of servo-controlled pods and the whole instrument is protected against changes in temperature and dust by a protective cover. The light is then propagated in the complete spectral range from 0.450 μm to 2.320 μm to the first dichroic beamsplitter that splits the light. The visible part of the spectrum is used for ZIMPOL, the near infrared (NIR) part of the spectrum for both IRDIS and IFS. If ZIMPOL is not used, all light goes to the wavefront sensor that is used by SAXO to correct for the aberrations of the light in the atmosphere. After the first dichroic beamsplitter, the light is guided through an atmospheric dispersion corrector (ADC) that corrects for dispersion effects in the atmosphere that are caused by the change in altitude of the object over time.

adaptive optics

SAXO is the adaptive optics module of SPHERE. It is composed out of different components, each correcting a part of the distortion of the light. The bundled information of these components is send to the deformable mirror (DM), that corrects for phase perturbations of up to a frequency of 1.2 kHz by use of the 41x41 actuators that are able to deform the mirror [21]. The phase perturbations are measured by different components.

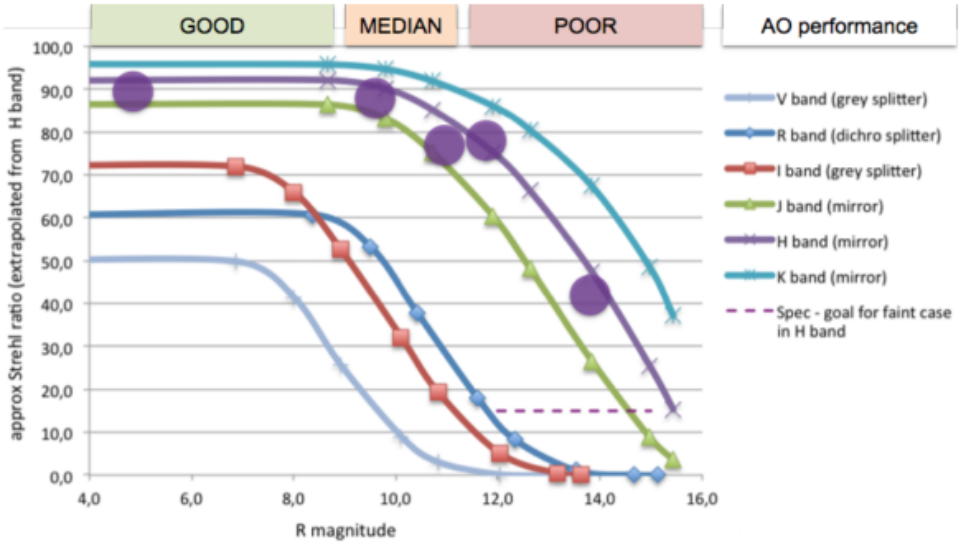

Figure 3.2: *Theoretical and measured (purple circles) SPHERE-SAXO Strehl ratio as a function of R magnitude for good seeing conditions and different wavelength ranges from V to K. Figure adapted from [22]*

The turbulence is measured by a wavefront sensor that transposes the phase shift to an intensity distribution on a detector. The wavefront sensor that is used is a Shack-Hartmann sensor [23]. This sensor uses a 40x40 lenslet array that produces a spot for each lenslet on a detector that has 240x240 pixels. A distorted incomming wavefront changes the position of the focal spot of the lenslets on the sensor, which can be used to calculate the local tilt of the wavefront. Other distorsions such as image motion and pupil shift are measured with tip tilt sensors, correcting only the large scale variations that these distorsions cause.

The incomming wavefront of the object is accurately corrected in a radius of about 20 λ/D in the image plane. Further out is the PSF still corrected, but not enough to suppress the stellar halo. The correction of the

AO is dependent on the magnitude in the R-band (618nm-674nm [24]), since the Shack-Hartmann sensor measures the perturbations of the wavefront in the range of the R filter. The more light is provided to the sensor, the more accurate the distorsions of the wavefront can be measured, which drastically changes the overall performance of the AO and hence the quality of the data. The performance of the AO as a function of R magnitude is illustrated in Figure 3.2, where the performace is expressed in terms of Strehl ratio. Strehl ratio is roughly defined as the ratio between the peak of the measured PSF divided by the peak of an ideal PSF.

coronagraphs

A coronagraph is a device that increases the contrast between the star in the center and the background. SPHERE has several coronagraphs for different conditions the instrument can work in. All coronagraphs consist of three components. At the begin of the light path an apodizer changes the beam profile and improves the dynamic range of the image that way. Further downstream in the focus of the secondary mirror, a focal plane

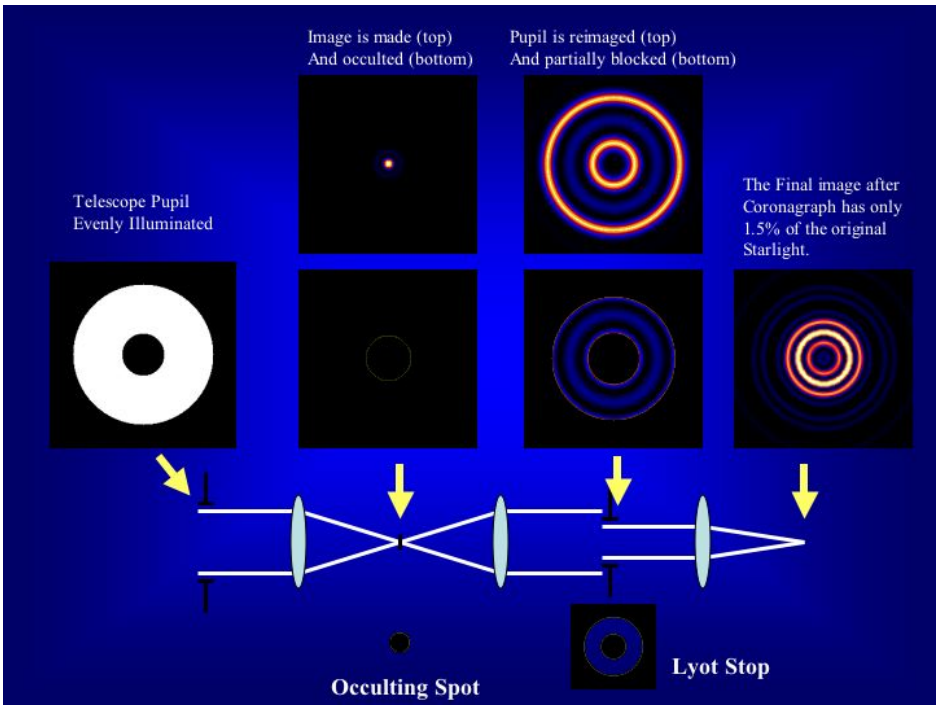

Figure 3.3: *Explanation of the working of a Lyot coronagraph. Figure adapted from [25]*

mask absorbs most of the light from the center of the beam such, that after reimaging the excess light of the center is concentrated around the edged of the telescope pupil. This excess light is absorbed by lyot stops that block most of the light on the edges of the beam, but allows light from surrounding sources to pass. Different combinations of these three elements have different results on the final image and all the combinations have conditions they work the best. Think of the wavelength range that is used at that moment, seeing and needed inner working angle. An elaborate explanation of the working of the coronagraphs in SPHERE is illustrated in Figure 3.3.

3.1.2 IRDIS

IRDIS has a field of view of 11”x12.5” and has several modes in which data can be acquired. The NIR part of the beam that is seperated by the first dichroic beamsplitter can be used in two different way. All the light can be reflected on a mirror to IRDIS, which provides classical imaging, dual band imaging, dual-polarization imaging with the filters Y to Ks and long slit spectroscopy. Another possibility is to use a second dichroic beamsplitter that allows to use both IRDIS and IFS for longer and shorter wavelengths respectively. Two different dichroic beamsplitters are possible in

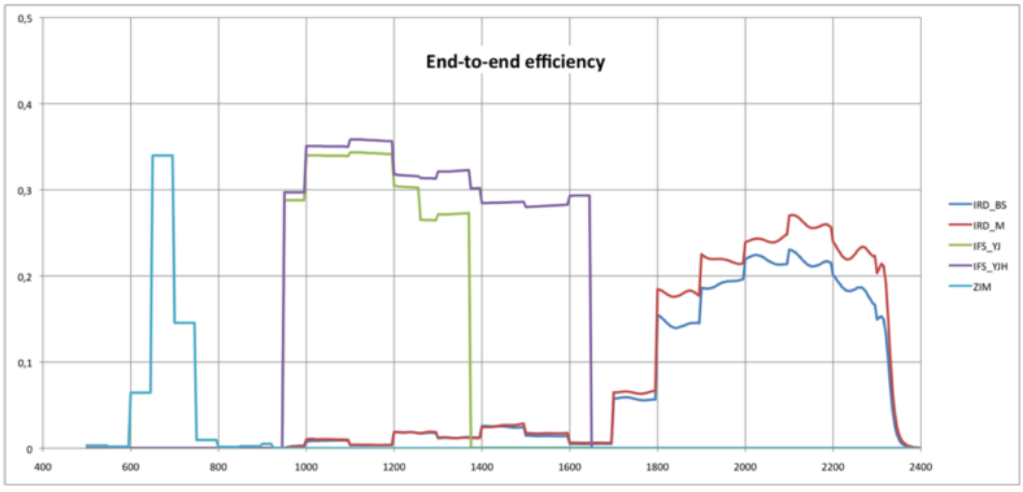

Figure 3.4: *End-to-end efficiency if both IFS and IRDIS get light. The light of ZIMPOL is in this case for the AO system. Note that only the IRDIS curves are shown in case the instrument is set up in IRDIFS_EXT mode. Figure adapted from [17]*

this case. If the instrument is set up in IRDIFS mode, the IFS receives light in the Y-J band and IRDIS is able to do narrow band or broad-band H Dual band imaging in parallel. In IRDIFS_EXT mode, the IFS receives light in the range from the Y band to H band, leaving IRDIS with the possibility to get dual band imaging data with lower efficiency in a narrow-band filter or in broad-band K. The end-to-end efficiencies of both possibilities are shown in Figure 3.4.

3.2 Integral Field spectrograph

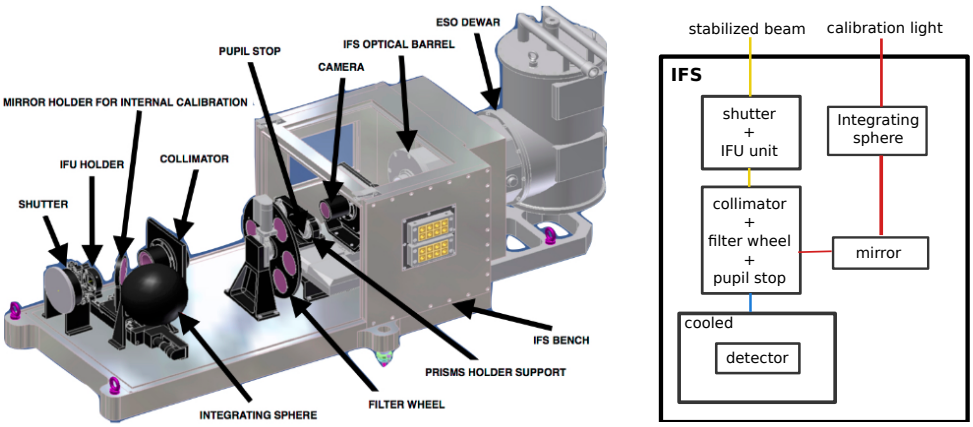

(a) *Figure adapted from [17]* ***(b)***

Figure 3.5: *overview of SPHERE/IFS*

The integral field spectrograph is a subsystem of SPHERE that is able to collect data over a wavelength range from 0.95 μm up to 1.346 μm or 1.677 μm, depending on the NIR dichroic beam splitter (Y-J or Y-H) is used. The spectral resolution of the IFS is on average R = 55.1 in Y-J mode and R = 34.5 in Y-H mode. The IFS has a total field of view of 1.73"x1.73", which is much smaller than IRDIS', but enough to be able to detect structures of protoplanetary disks close to the star.

3.2.1 IFU unit

The IFS is able to obtain spectral information by use of BIGRE [26], an integral field unit consisting of 122x122 microlenslets with a diameter of 150 μm, in a hexagonal grid, as illustrated in Figure 3.7. This grid is rotated by 10.7^o with respect to the dispersion in order to get the most lenslets

stacked on the grid. This results in a small section of the detector to be meaningless, as illustrated in Figure 3.6. The FWHM of these spectra is at the middle of the spectral range 29.6 mas. The spatial sample scale of the detector is 12.3 mas, which increases the angular resolution, but has still a high signal to noise ratio on the detector. The spectra of these lenslets are projected on the detector in a rectangular area with dimensions 5.1x41 pixels [5].

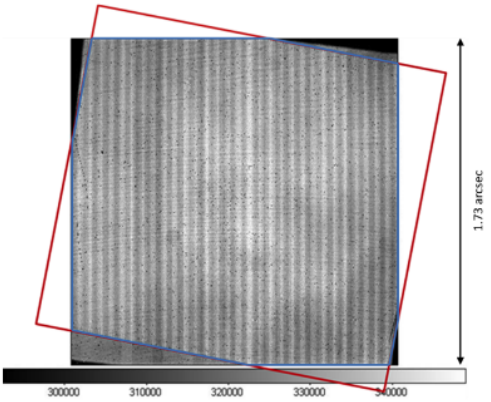

Figure 3.6: *IFS flat-field and projection of the sky. In the red the arrangement on the BIGRE detector and in blue the useful FOV. Figure adapted from [17]*

3.2.2 Detector

The detector of the IFS is 2048x2048 pixels big, each pixel corresponding to $(7.46 \text{ mas})^2$. The incomming light of the IFS is filtered by an additional filter that has a sharp cut-off at the desired wavelength, which allows the de-

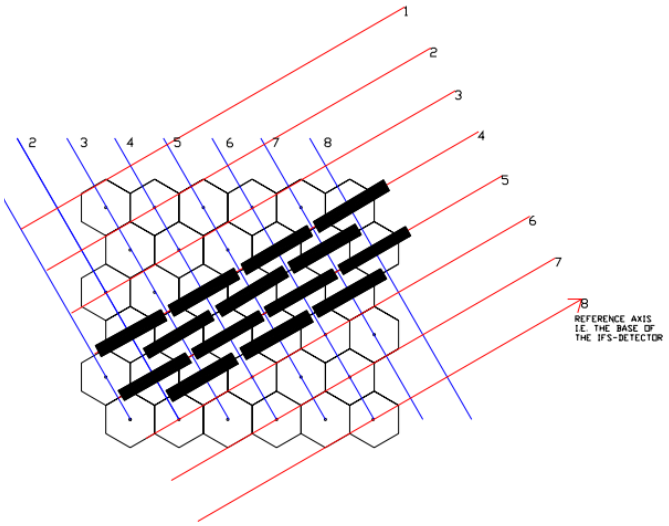

Figure 3.7: *The hexagonal lines represent the different microlenses of the IFU, the solid rectangles represent the spectra of the lenslets on the detector, the numbered lines represent the orientation of the IFS Detector. Figure adapted from [5]*

tector to be a standard infrared detector. It is technically possible to block longer wavelengths by use of the cut-off wavelength at which an HgCdTe detector is no longer sensitive, but this would make the instrument unnecassary complex and would increase the readout noise drastically from 10 e^- to 25 e^- [5]. This cut-off allows cooling only the detector, but keeping the optics at room temperature, since the contribution of the thermal background to the noise is neglectable since all radiation at wavelengths longer than 1.35 μm is blocked. The detector is cooled with liquid Nitrogen, which reduces the thermal noise of the detector[5]. The detector is static and does not need to be rotatable since the rotation of the field and the pupil are corrected in the derotator.

3.2.3 Calibration devices

The IFS has two calibration arms to provide a proper calibration of the instrument. The first arm is mounted in the common path and consists of a few calibration lamps. These lamps can be used to measure the throughput of the lenslet grid and the different optical components of the IFS. Four additional lasers with wavelengths of respectively 0.9877, 1.1237, 1.3094 and 1.5451(μm) are also provided on this calibration arm for the wavelength calibration. Each of the lasers is focused on a different part in the spectra on the detector by the IFU. Interpolation between these points gives an accurate model for the wavelength solution for each pixel, which can be used to reduce the data.

The second calibration arm is mounted internal to IFS, after the IFU, such that flats can be taken that measure the sensitivity of the whole detector. This is not possible with the external calibration lamps, since the detector has bigger dimensions than the FOV of the lenslet grid. Decoupling the noise of the IFU and the detector makes the calibration slightly better and this allows to take calibration frames in parallel with IRDIS taking calibration frames, making the calibration process for both subsystems much faster. The internal calibration arm consists out of five calibration lamps: four narrowband lamps, centered around 1.0, 1.2, 1.3 and 1.5 μm, with a full width half maximum (FWHM) of about 0.01-0.04 μm and one broadband white lamp[27]. An integrating sphere is also provided that spreads the light of the different lamps evenly over the whole detector. An elaborated description of the different calibration steps is given in the methodology chapter.